

# CONTINUUM AND DISCONTINUUM MODELLING IN TUNNEL ENGINEERING

Prof. dr. eng. sc. Giovanni Barla, Dr.geot. eng. Marco Barla,  
Dept. of Structural and Geotechnical Engineering, Politecnico di Torino, Italy

**SUMMARY:** The paper discusses continuum and discontinuum modelling in tunnel engineering. A brief review of fundamentals is presented in connection with the use of closed-form solutions and computer based numerical methods. A few remarks are derived on the choice of either continuum or discontinuum modelling of rock mass behaviour at the design analysis stage. Consideration is given to the validation of discontinuum modelling in connection with rock mass classification methods and expected tunnel response to excavation. A case study of a TBM tunnel (4.75 m diameter) in quartzitic micaschists is discussed in detail by paying attention to a comparison of modelling methods – including continuum and discontinuum modeling – applied at a fault zone.

## 1. INTRODUCTION

The prediction of the rock mass response to the excavation of a tunnel is a complex engineering problem. The interest of the Rock Engineer at the design stage is to assess the stability conditions of the excavation in the "intrinsic state" (i.e. when no support/stabilization measures are installed) and following the adoption of suitable methods of tunnel excavation/construction and support. The key to the success of such a process is the level of understanding achieved in describing the rock mass conditions (in terms of geological, geotechnical, in situ stress, and hydrogeological parameters) and the ability to account for the fundamental components of rock mass behaviour, by using appropriate methods for the analysis of stresses and displacements in the rock mass around the tunnel and in the structural components (pre-support/pre-stabilization measures; primary and final support, etc.).

A number of methods are available for the stress analysis of tunnels, from the earliest closed-form solutions to the most recent numerical modelling methods. With the computational power today available at a reasonable cost, it is possible to solve increasingly sophisticated problems. In particular, with the advent of numerical methods, we have assisted to the development of techniques which have been conceived to model realistically the rock mass behaviour. This is a quite different condition from the early start of Rock Mechanics, when the methods of analysis and the solutions used were mostly taken from other engineering disciplines. This is certainly the case of the 1898 Kirsch solution for the stresses and displacements around a circular hole in a biaxially loaded, homogeneous, isotropic and linearly elastic plate.

Closed-form solutions are still of great value for a conceptual understanding of the response of tunnels to excavation. One could mention in this

regard the solutions which are presently available for the analysis of the progressive development of failure around a circular tunnel in a hydrostatic stress field (see for example: Brown et al., 1983; Panet, 1995), and for the analysis of the interaction between the rock mass and the support. However, the development of modern techniques of tunnel excavation and construction (i.e. the case of pre-support/pre-stabilization measures, the frequent adoption of pre-treatment ahead of the heading in weak rock masses, the excavation sequences, typical of large tunnels), ... and even the complexity of rock mass conditions and behaviour, which are better described today than in the past, given the modern investigation tools available, etc. make these solutions of limited value for design purposes.

If we restrict our attention to modern numerical modelling methods and rigorous analysis of tunnelling problems, the decision that the Rock Engineer need to make at the design analysis stage is the choice between the following two approaches:

- Equivalent continuum approach: the rock mass is treated as a continuum with equal in all directions input data for the strength and deformability properties, which define a given constitutive relation for the medium: elastic, elasto-plastic, etc.
- Discontinuum approach: the rock mass is represented as a discontinuum and most of the attention at the design stage is devoted to the characterization of the rock elements, the rock joints and discontinuities. The modelling approach consists in considering the blocky nature of the system being analysed. Each block may interact with the neighbouring blocks through the joints. The interest lies in the fact that the fundamental patterns of rock mass behaviour can be considered, as arbitrarily large relative displacements may take place at the contacts.

This lecture is intended to discuss a comparison of modelling methods – including continuum and discontinuum modelling – applied at a fault zone in a TBM tunnel. Reference is made to a paper recently presented at the 9<sup>th</sup> International Congress on Rock Mechanics in Paris (Barla G et al., 1999).

## 2. FUNDAMENTALS

### 2.1. Continuum versus discontinuum modelling

#### 2.1.1. Continuum modelling

The use of continuum modelling in tunnel engineering makes it essential to simulate the rock mass response to excavation by introducing an equivalent continuum. The most common way to solve this problem, which seems to have gained wide acceptance, is to scale the intact rock properties down to the rock mass properties by using empirically defined relationships such as those given by Hoek and Brown (1997).

If use is made of the Hoek-Brown criterion for describing the rock mass behaviour, the starting point of the scaling process is the definition of the intact rock material parameters such as  $\sigma_{ci}$  (uniaxial compressive strength) and  $m$  (material constant which depends upon the properties of the rock), which can be obtained based upon the results of uniaxial and triaxial laboratory testing. Then, by using well known correlations (which depend on the degree of disturbance to the rock which will vary according to rock type and excavation method) with the most frequently adopted rock mass indices (i.e. truncated Q or RMR values, or GSI values), the rock mass parameters such as  $m_b$  and  $s_b$  (rock mass constants according to the Hoek-Brown criterion) or  $c$  and  $\phi$  (rock mass cohesion and friction angle respectively) can be estimated (Figure 1).

The next step in the continuum modelling approach is the adoption of the appropriate constitutive relations for the rock mass. Linear elasticity is commonly used, although nonlinear elastic constitutive equations can also be adopted. If the attention is posed on the progressive failure of the rock mass, the elasto-plastic models need to be utilized in order to describe the "post-peak" response. A yield function which is often chosen coincides with the Hoek-Brown failure criterion: (i) the rock mass response is elastic, if the state of stress is within the bounds defined by the yield function; (ii) the rock mass response is plastic, once the state of stress is such as to reach the yield function. A number of "post-peak" responses may be postulated depending upon rock mass quality; the characteristics shown in Figure 2 are among the most frequently used for the solution of tunnelling problems (Hoek and Brown, 1997):

- Very poor quality rock mass: the rock mass behaviour is adequately represented by assuming that it behaves perfectly plastic, which means that deformation continues at a constant stress level and that no volume change is associated with the ongoing failure.
- Average quality rock mass: it is reasonable to assume that a strain-softening behaviour occurs as the rock mass strength is reduced from the in situ to the broken state; then, once this final, "residual" state is reached, deformation will occur at a constant stress level.
- Very good quality hard rock mass: in such a case (hard rock masses, such as massive granites and gneiss) it is assumed that, when the rock mass strength is exceeded, a sudden strength drop occurs.

This is associated with significant dilation of the rock mass, which is considered to behave as a medium with zero cohesive strength and finite friction angle.

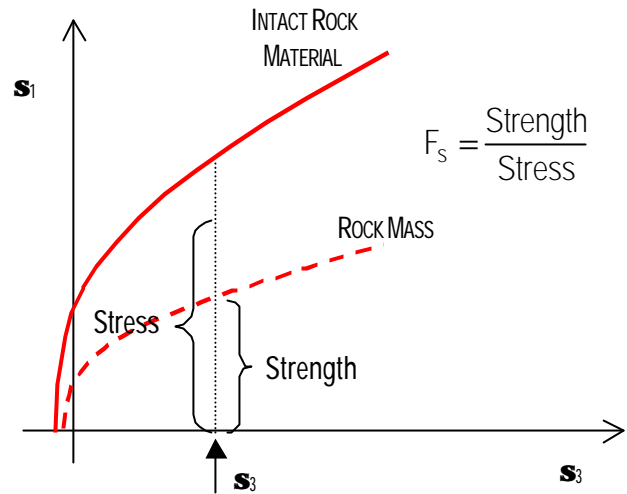


Figure 1. Hoek-Brown failure criteria for the intact rock material and the rock mass. Illustration of the scaling process and definition of Factor of Safety.

As summarized by Hoek et al. (1991) - also see Startfield and Cundall (1988) - a number of computer-based numerical methods have been developed over the past few decades and these provide the means for obtaining appropriate solutions to tunnel engineering problems in the framework of the equivalent continuum approach. These numerical methods can be divided into two classes: boundary and domain methods. The boundary methods comprise several types of boundary element methods (BEM) and imply the subdivision of the boundary of the excavation into elements, as the interior of the rock mass is represented mathematically as an infinite continuum. The domain methods, which include the finite element (FEM) and finite difference methods (FDM), imply that a physical problem is modelled numerically by discretizing (i.e. dividing into zones or elements) the problem region, i.e. the rock mass in which the excavation is to be created.

#### 2.1.2. Discontinuum modelling

With the understanding that rock joints and discontinuities in a rock mass play a key role in the response of a tunnel to excavation, i.e. joints can create loose blocks near the tunnel profile and cause local instability; joints weaken the rock and enlarge the displacement zone caused by excavation; joints change the water flow system in the vicinity of the excavation (see, for example: Shen and Barton, 1997), the use of discontinuum modelling has been gaining progressive attention in tunnel engineering mainly through the use of the UDEC and 3DEC codes, for 2D and 3D discontinuum modelling respectively. However discontinuum modelling is not being used as extensively as continuum methods and is considered to be a relatively new and "not-yet-proven" numerical technique to apply for analysis and design in rock engineering projects (Hart, 1993).

In the distinct element method, the rock mass is represented as an assemblage of discrete blocks which may be considered either "not deformed"

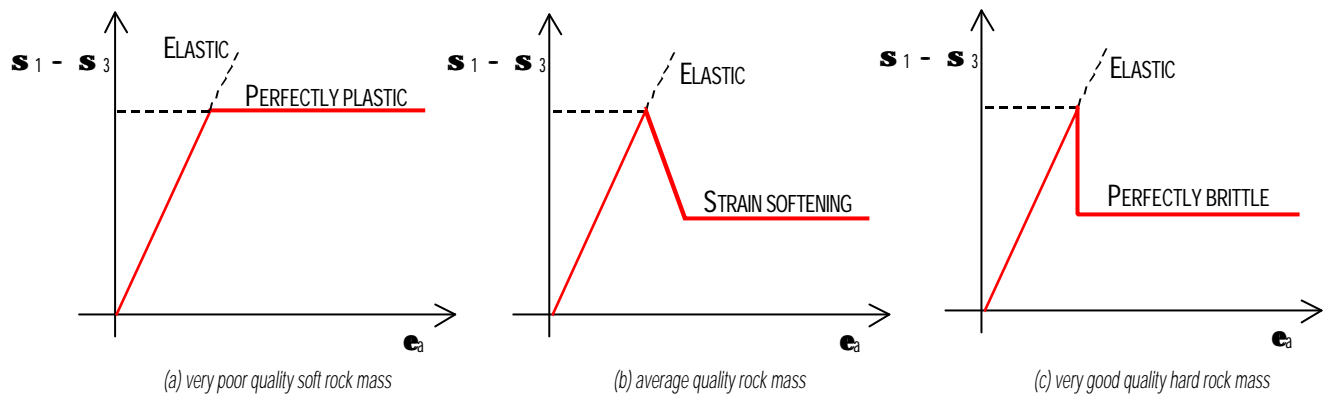


Figure 2. Suggested stress-strain laws for different quality rock masses, note that the stress scales are different (Hoek and Brown, 1997, modified).

mable" or "deformable". Joints and discontinuities are viewed as interfaces between distinct bodies. The important features of this method which make it appropriate in order to capture the important mechanisms characterising a discontinuous medium are (Cundall and Hart, 1993): (i) the method allows finite displacements detachment; (ii) the method recognizes new contacts automatically as the calculation progresses.

In order to apply the distinct element method to the solution of tunnel problems, there are two crucial issues which include the joint geometry data and the material properties assigned to the joints. The first issue relates to the introduction in the model of those joints which are most critical to the response of the rock mass. The second issue is closely connected with the need to assign to the joints in the model the stiffness and strength properties of the real joints in situ. Although published data are readily available in the specialised literature which may provide a way to guide into the choice of appropriate parameters (Bandis, 1993), this aspect of modelling still remains difficult. However, it is to be remarked that a significant help in deriving the necessary input data for 2D and 3D discontinuum modelling may be obtained from index testing of joints in drill cores and from field mapping (Barton, 1998 and 1999).

### 2.1.3. Discussion

When investigating a particular problem at the design analysis stage the decision is to choose between continuum and discontinuum modelling of rock mass behaviour. This decision may be based on the analysis of the likely mechanism (sliding along joints, opening of joints, block rotation and movement, etc.) which may influence tunnel stability and the joint spacing relative to the size of the excavation. Consideration may be given to a suggested range of  $Q$ -values for which discontinuum modelling will be more appropriate than continuum modelling ( $Q \cong 0.1 - 100$ ) as depicted in Figure 3 (Barton, 1998).

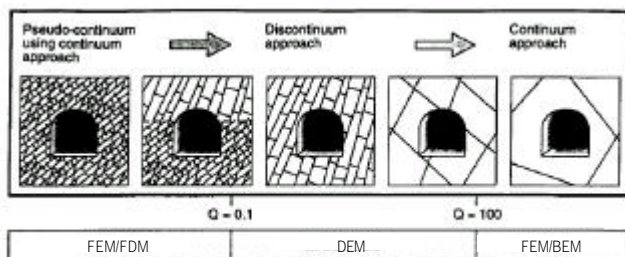


Figure 3. Schematic diagram suggesting the range of application of discontinuum modelling in relation to the  $Q$ -value (Barton, 1998, modified).

Based upon experience gained so far and a close scrutiny of design analyses which are sometimes used in tunnel engineering (), the following observations can be derived:

- Isotropic continuum modelling is being used more frequently than discontinuum modelling, even in cases where the block size is significant, compared to the size of excavation or the rock mass exhibits a strong anisotropic behaviour.
- Numerical modelling is being used too often, even in cases where problems are characterised by low levels of both input data and understanding (it is appropriate to recall the classification of modelling problems reported by Startfield and Cundall, 1988, who recognize this to be the case of most rock mechanics problems), or the size of the planned excavation is such as not to justify this exercise.
- It appears that the easy access to computer codes, which make sophisticated methods of analysis promptly available, may result in misuse of these methods. Sometimes, the tendency is to be happy with having run a model, even if the results obtained are in open contradiction with empirical design rules and engineering judgement.

### 2.2. Validation of discontinuum modelling

The use of numerical modelling in engineering practice, connected with the need to adopt modelling schemes (continuum versus discontinuum modelling) which are the most appropriate in order to analyse a given problem (provided that sufficient data are available), points out that "the modelling of the components, rock, rock joints and discontinuities is far more logical and relevant than present "black box" continuum models" (Barton, 1999). The comparison shown in Figure 4 well demonstrates this point of view, especially if critical mechanisms of the physical problem under study are to be included in the analysis.

\* The senior author derives these observations through experience gained in reviewing a number of design analyses carried out in Italy and abroad, in connection with hydroelectric, highways and high-speed railways projects.

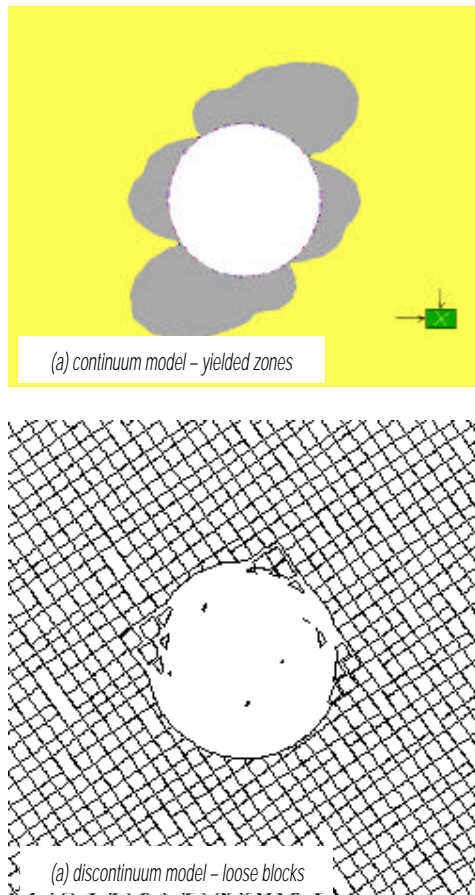


Figure 4. Comparison of (a) continuum ubiquitous joints case and (b) discontinuum modelling results when analysing typical instability mechanisms around a TBM excavated tunnel in a weak rock mass.

There is a relevant question which arises with reference to the use of discontinuum modelling in tunnel engineering and rock engineering, in general. This is in relation to the complexity of the discontinuum model to be used in order to be certain that the critical structural features have not been left out of the analysis (Hart, 1993). From one side, the difficulty is in providing sufficient geological data; from the other side, the computer hardware requirements may exceed that available.

Based on the experience gained so far, a possible approach to this problem consists in using discontinuum modelling in connection with rock mass classification methods in a framework of cross-validation of the expected tunnel response to excavation. Once the specific model has been proven to be acceptable in a given rock mass condition, it may be improved and further validated during tunnel excavation. A set of guidelines, given as a function of  $Q$  values, can be used as a form of preliminary verification of a numerical model (Barton, 1999).

#### - Support categories

Based upon analyses of case records, Grimstad and Barton (1993) give the diagram of Figure 5 which allows one to relate the value of the index  $Q$  to the stability and support requirements of underground excavation, once the parameter which they called Equivalent Dimension is obtained. This parameter is the span, diameter or wall height of the same excavation divided

by a numerical coefficient which is intended to account for its use and the degree of security which is demanded of the support system installed to maintain the stability of the excavation.

Additional guidelines are available based on the  $Q$  system which allow one to assess a number of additional parameters dealing with tunnel stability and support requirements (Barton et al., 1974): a) the maximum unsupported span, b) the permanent roof support pressure; c) the bolt length.

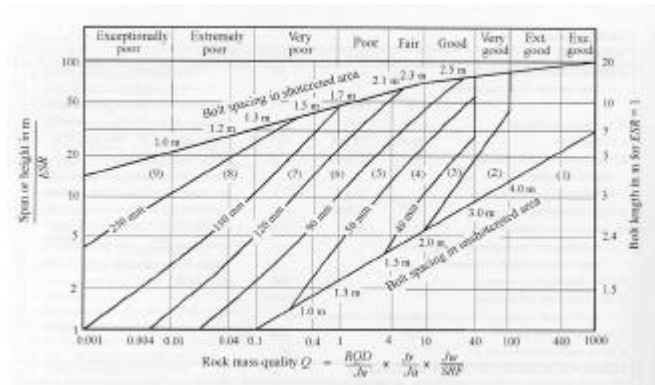


Figure 5. Estimated support categories based upon the tunnelling quality index  $Q$  (Grimstad and Barton, 1993).

#### - Tunnel deformation (Barton, 1998)

$$\text{Vertical: } \Delta v = \frac{\text{SPAN}}{100 \cdot Q} \sqrt{\frac{s_v}{s_c}} \quad [\text{mm}]$$

$$\text{Horizontal: } \Delta h = \frac{\text{HEIGHT}}{100 \cdot Q} \sqrt{\frac{s_h}{s_c}} \quad [\text{mm}]$$

where:  $s_v$  and  $s_h$  (the vertical and horizontal in situ stress components),  $s_c$  (the uniaxial compressive strength of the intact rock material) are given in consistent units (i.e. MPa); SPAN and HEIGHT (the width and height of the tunnel) are given in mm.

#### 2.2.1. Case Examples

With the case history in mind, which is to be discussed in the following, a 4.75 m diameter tunnel was taken as a typical problem to be used for validation of the discontinuum modelling by the 2D Distinct Element code UDEC (Itasca, 1996). The intent has been to investigate the influence of rock mass conditions by the  $Q$  index, on the disturbed zone around the tunnel.



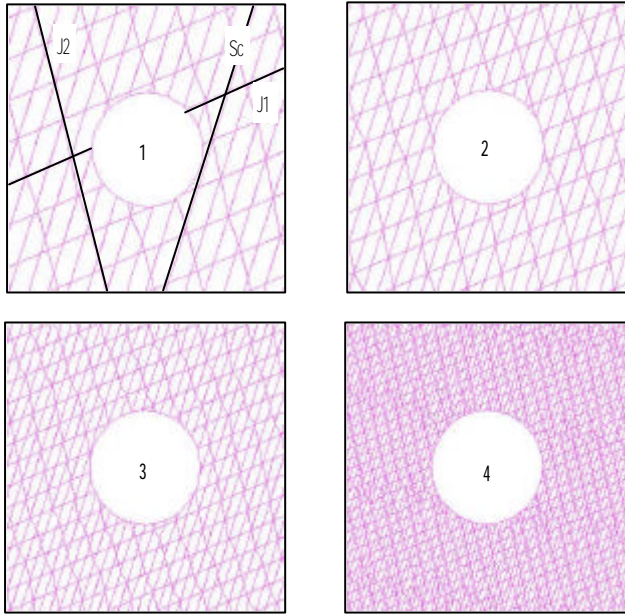


Figure 6. Four UDEC models with different  $Q$  values: model 1 –  $Q=8.5$ ; model 2 –  $Q=4.1$ ; model 3 –  $Q=1.9$ ; model 4 –  $Q=0.67$ .

Four models have been used as shown in Figure 6. With dimensions 20x20 m, three sets of persistent discontinuities ( $S_c$  = schistosity, J1, J2 joints) have been introduced with the parameters assigned so as to obtain a range of  $Q$  values from 8.5 for model 1 to 0.67 for model 4. For all the models the initial state of stress is assumed to be given by:  $\sigma_v$  (vertical stress) = 16.2 MPa,  $\sigma_h$  (horizontal stress) = 4 MPa, which represent a gravity induced stress state at a depth of about 600 m, with an assumed stress ratio ( $\sigma_h/\sigma_v$ ) of 0.25. The joint spacing for each system shown in Figure 6 is as follows:

| Model | Schistosity | JOINT SPACING (m) |     |
|-------|-------------|-------------------|-----|
|       |             | J1                | J2  |
| 1     | 0.8         | 1.6               | 2.0 |
| 2     | 0.6         | 1.2               | 1.5 |
| 3     | 0.4         | 0.8               | 1.0 |
| 4     | 0.2         | 0.4               | 0.5 |

For all the models the rock blocks are deformable blocks with the assumption that the intact rock (gneiss) is considered as an elasto-plastic material which follows the Mohr-Coulomb yield criterion. The properties are assigned as follows:

|                 |                      |
|-----------------|----------------------|
| Young's modulus | $E = 60 \text{ GPa}$ |
| Poisson's ratio | $\nu = 0.25$         |
| Cohesion        | $c = 30 \text{ MPa}$ |
| Friction angle  | $\phi = 33^\circ$    |

The discontinuities are assumed to be Mohr-Coulomb joints, i.e. elasto-perfectly plastic joints, with normal  $K_n$  and shear  $K_s$  stiffness given as follows:  $K_n = 40 \text{ GPa/m}$ ,  $K_s = 4 \text{ GPa/m}$ . The cohesion is always considered

to be zero, with the friction angle  $\phi$  taken as  $58^\circ$ ,  $38^\circ$ ,  $22^\circ$  and  $11^\circ$  respectively for models 1, 2, 3 and 4, for both the schistosity and joints.

#### - Unsupported tunnel

A first series of analyses was carried out in intrinsic conditions, i.e. the tunnel is always left unsupported, with the disturbed zone defined as follows (Shen and Barton, 1997):

- failure zone, where loose rock blocks are falling into the tunnel;
- open zone, where joints open up;
- shear zone, where joints experience a certain shear displacement (3 mm).

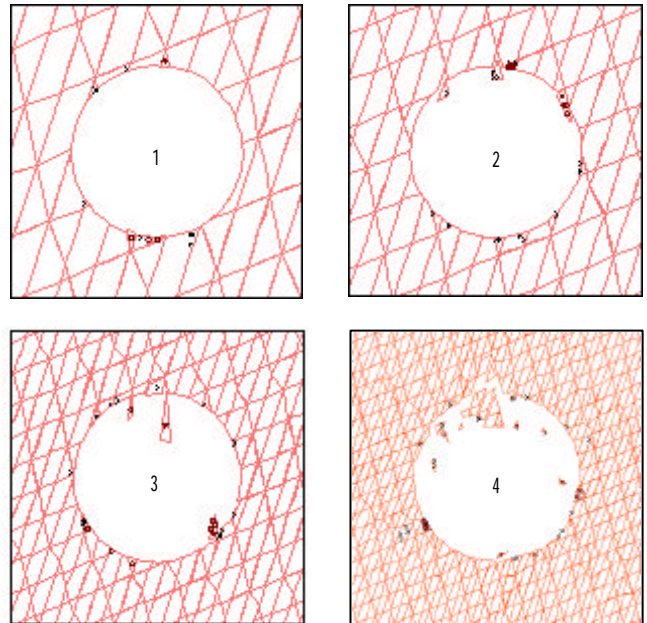


Figure 7. Yielded and loose blocks around the tunnel for models 1 to 4.

The results obtained for the 4 models, are illustrated in Figures 7 to 9, where the failure, open and shear zones around the tunnel are depicted. The following remarks are made: (1) the failure zones computed around the tunnel show that model 1 is stable, whereas models 2 to 4 exhibit progressively critical conditions; (2) the open and shear zones appear to grow as the rock mass quality decreases from model 1 to 4, in line with the behaviour in terms of failure zones; (3) the results obtained seem to agree with the estimated support categories shown in Figure 5, where only the tunnel simulated with model 1 would require no support, and models 2 to 4 would need different and progressively more severe support measures.

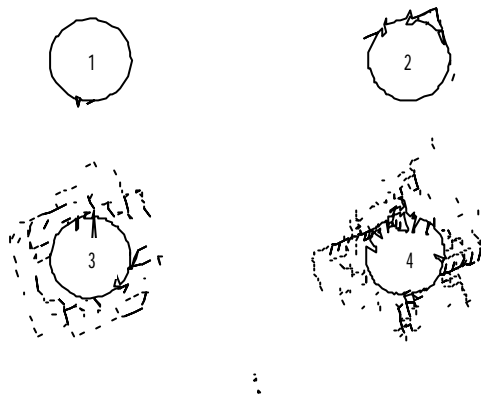


Figure 8. Open zones around the tunnel for models 1 to 4.

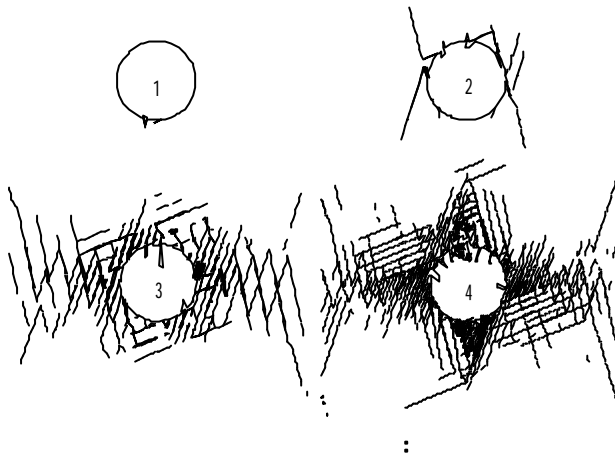


Figure 9. Shear zones around the tunnel for models 1 to 4.

#### - Supported tunnel

As a direct consequence of the analyses described above and based upon the guidelines of Figure 5 in terms of support requirements, the following stabilization measures were introduced in models 2 to 4:

| Model | Bolts n. | Bolt length<br>[m] | Bolt spacing <sup>(1)</sup><br>[m] | Shotcrete thickness<br>[cm] |
|-------|----------|--------------------|------------------------------------|-----------------------------|
| 2     | 5        | 2.4                | 1.70                               | 4.0                         |
| 3     | 9        | 3.0                | 1.40                               | 8.0                         |
| 4     | 11       | 3.0                | 1.25                               | 11.5                        |

<sup>(1)</sup> Bolts are supposed to be installed according to a square pattern.

The bolts were simulated by using the CABLE option available within the UDEC code, which allows one to consider a bolt fully bonded to the rock mass. The shotcrete was introduced in the model by the STRUCT option which consists in simulating it as a series of beams connected to the rock mass.

As a first estimate of the predictive capability of the UDEC discontinuum modelling of the supported tunnel the attention is posed on comparing the vertical and horizontal displacements  $\Delta v$  and  $\Delta h$  given by the empirical Q based formulae reported above and the results of UDEC computations:

| Model | $\Delta v$ [mm]<br>estimated-computed | $\Delta h$ [mm]<br>estimated-computed |
|-------|---------------------------------------|---------------------------------------|
| 2     | 4.5 – 5.0                             | 2.6 – 2.6                             |
| 3     | 9.2 – 10.2                            | 4.7 – 5.3                             |
| 4     | 26.0 – 25.1                           | 13.3 – 12.9                           |

### 3. CASE STUDY

#### 3.1. Background information

The case study considers the problems occurred on 11 September 1997, at ch 2360 m, when crossing a fault zone which caused the TBM to become temporarily stuck during excavation of the F2 tunnel, one of the major element of the Pont Ventoux - Susa Hydropower Project in the Susa Valley, near Torino. This tunnel (4.75 m diameter) is being excavated by an open TBM configuration through quartzitic micaschists under a cover which is to reach 800 m maximum (Figure 10).

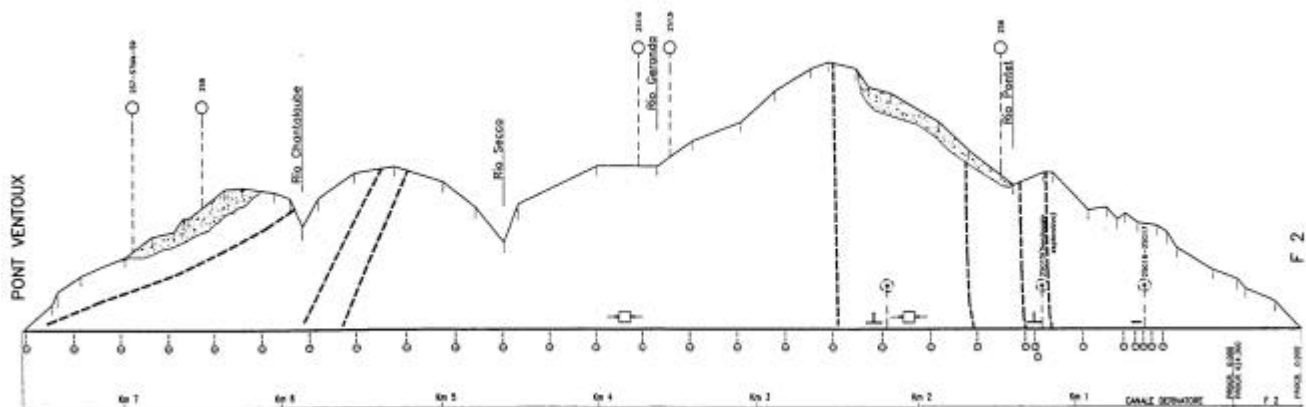


Figure 10. Pont Ventoux - Clarea F2 tunnel.



Figure 11. A view of the F2 tunnel in the section where the gneiss rock mass was generally good.

Following the first 1800 m approximately where the rock mass conditions were generally good, with RMR values ranging from 65 to 75 (Figure 11), TBM tunnelling in the F2 tunnel became progressively more severe with the approaching of the fault zone. At present, the tunnel is experiencing very severe difficulties with considerable delays with respect to the expected advance rate. Figure 12 shows two photographs taken following chainage 2360 m, where the fault of interest in this paper crossed the tunnel, affecting progress significantly.

### 3.2. Description of the overstress problem at ch 2360 m.

The sketch shown in Figure 13 gives a simplified illustration of the conditions at the tunnel face where the TBM became temporarily stuck as a consequence of overstressing and a 25 cm block movement of the right sidewall (Figure 14). The quartzitic micaschist is characterized by the presence of three to four joint systems including foliation. Based on geologic mapping, which was carried out by the contractor's geologist (Pont Ventoux, 1997) once the TBM could drill a few meters ahead of the section where it jammed (Figure 15), at least two sub-parallel discontinuities could be evidenced, the second of which (a fault with strike N66E and dip 83 to

the S, which intercepts the tunnel axis) has a clay filling and gouge with aperture ranging from a few centimeters to more than a decimeter.

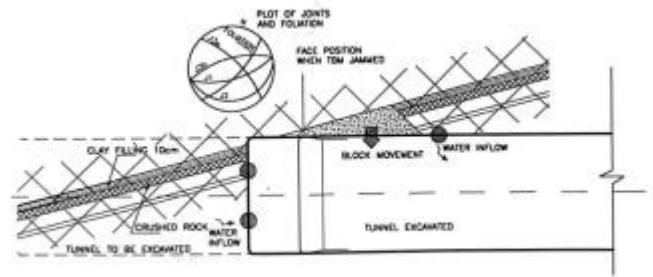


Figure 13. Sketch of the rock conditions at the face.



Figure 14. Photograph showing the head of TBM jammed with rock overstressing and block movement of the right sidewall.



Figure 12. A view of the F2 tunnel: (a) left (b) right walls, where stability conditions became very difficult so as to require continuous placement of liner plates.

The rock mass conditions were estimated on a 7 m tunnel length, from ch 2349 to ch 2356 m, with RMR index equal to 31. According to a more complete Q-logging estimate due to Barton (1997), from ch 2350 to ch 2360 m, an extreme range of Q-values of about 0.007 ("exceptionally poor" - b- cally) to 0.3 ("poor") showed a weighted mean of all recordings of about 0.05. Water is flowing through the joints at a temperature of 20°. No quantitative data have been recorded of the water pressure, which seems unlikely to be exceeding, with an overburden of 650 m, a maximum of 6 to 7 Mpa (outside the tunnel drainage area).

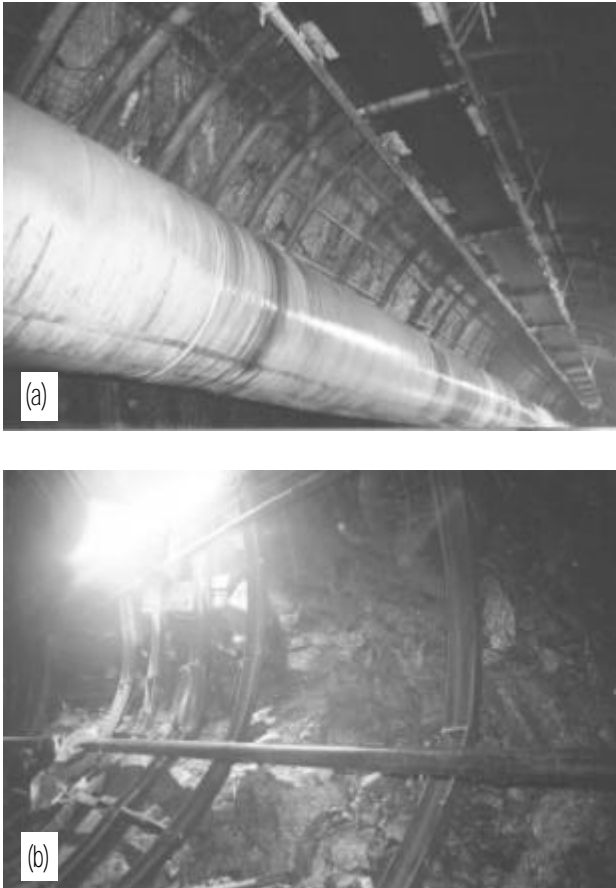


Figure 15. Rock mass conditions on the tunnel (a) left (b) right walls. The photograph was taken when the TBM was moved ahead.

### 3.3. Rock mass strength

The rock mass strength in the section of interest is largely controlled by the generally "poor" conditions and the limited shear strength along discontinuities. Typical strength properties derived from triaxial testing of rock samples are as follows:

|                |                |           |           |
|----------------|----------------|-----------|-----------|
| $\sigma_{c,p}$ | $\sigma_{c,r}$ | $m_{i,p}$ | $m_{i,r}$ |
| [MPa]          | [MPa]          | [-]       | [-]       |
| 144            | 77             | 7.0       | 6.1       |

where  $\sigma_{c,p}$  and  $\sigma_{c,r}$  are the uniaxial compressive strength values (peak and residual) and  $m_{i,p}$  and  $m_{i,r}$  are the corresponding Hoek-Brown empirical constants.

For very good quality rock masses, which is the case for a significant tunnel length (Figure 11), typical rock mass properties can be defined on the basis of the Geological Strength Index (GSI) as follows:

|                                |                          |
|--------------------------------|--------------------------|
| Intact rock strength           | $\sigma_{ci} = 144$ MPa  |
| Hoek-Brown constant            | $m_i = 7.0$              |
| Geological Strength Index      | GSI = 70                 |
| Hoek-Brown constant            | $m_b = 2.4$              |
| Hoek-Brown constant            | $s = 0.02$               |
| Rock mass compressive strength | $\sigma_{cm} = 27.2$ MPa |
| Deformation modulus            | $E_m = 35$ GPa           |

### 3.4. In situ stress conditions

In view of the high overburden and closer valley side, associated with evidence of deformation and thin slabbing in isolated sections along the tunnel length, it was recommended that stress measurements by means of flat-jack tests and hydraulic minifracure tests be carried out. At present only the flat-jack test data are available as follows, derived from measurements around the section of the tunnel at ch 950 m, where the overburden is approximately 400 m:

| Flat-jack slot | Angle with respect to horizontal axis | Jack pressure |
|----------------|---------------------------------------|---------------|
|                | [°]                                   | [MPa]         |
| M1             | 0                                     | 34.8          |
| M2             | +50                                   | 3.3           |
| M3             | -45                                   | 23.5          |

Based on a stress concentration study in linearly elastic conditions around the tunnel using the finite element method and the Phase<sup>2</sup> code (Curran and Corkun, 1997), as shown in Figure 16, the initial stresses in the plane perpendicular to the tunnel axis were evaluated to be as follows:

- $\sigma_1$  = maximum principal stress = 13 MPa
- $\sigma_3$  = minimum principal stress = 2.6 MPa
- $\theta_1$  = angle of  $\sigma_1$  with respect to the vertical axis = 15°



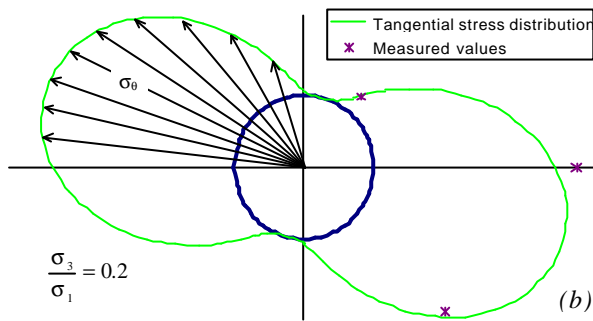
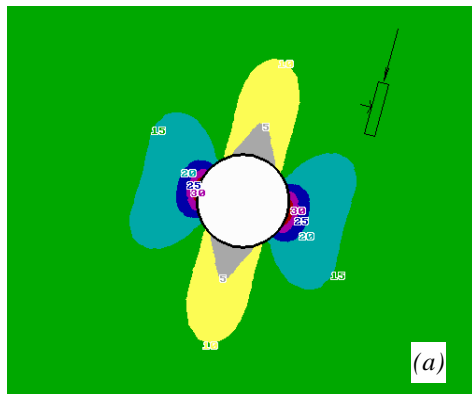


Figure 16. (a) Maximum principal stress contours. (b) Computed and measured tangential stresses. Flat-jack slot tests, with overburden of 400 m approximately.

### 3.5. Continuum modelling

#### 3.5.1. The $m = 0$ approach

In order to determine to what extent the adoption of a continuum modelling approach can provide a reasonable interpretation of tunnel instability, numerical analyses were first carried out to assess the stability conditions by using a constant deviatoric stress criterion as proposed by Martin et al. (1997).

The initial stresses  $\sigma_1$  and  $\sigma_3$  at the cross section of interest (ch 2360 m) were assumed to be proportionally higher in relation to the higher overburden of 650 m. Also, the stress ratio ( $K_0$ ) of the minimum stress to maximum stress ( $\sigma_3/\sigma_1$ ) in the plane of the tunnel cross section was considered equal to 0.2, as in the section of the flat jack measurements.

The  $m = 0$  analyses were performed by using the Phases<sup>2</sup> code and the Hoek-Brown criterion for different values of  $\sigma_{ci}$  and  $s = 1$ . The stability of the tunnel was assessed by computation of the strength factor contours as shown in Figure 17. The implication is that the rock mass inside the unit strength factor contour ( $SF_{(m=0)} = 1$ ) will be unstable, unless well retained.

From the above simplified analyses (continuum linearly elastic constitutive model, no influence of hydrostatic head considered, etc.) the tunnel experiences localized failure at the sidewalls which deepens inside the rock mass as the micaceous intact rock uniaxial compressive strength decreases from 100 MPa to 75 MPa. This would signify that in the highly anisotropic stress regime of the tunnel, as evidenced with a  $K_0$  value equal to

0.2, localized slabbing instability cannot be ruled out, if the rock strength is in the range 100-75 MPa.

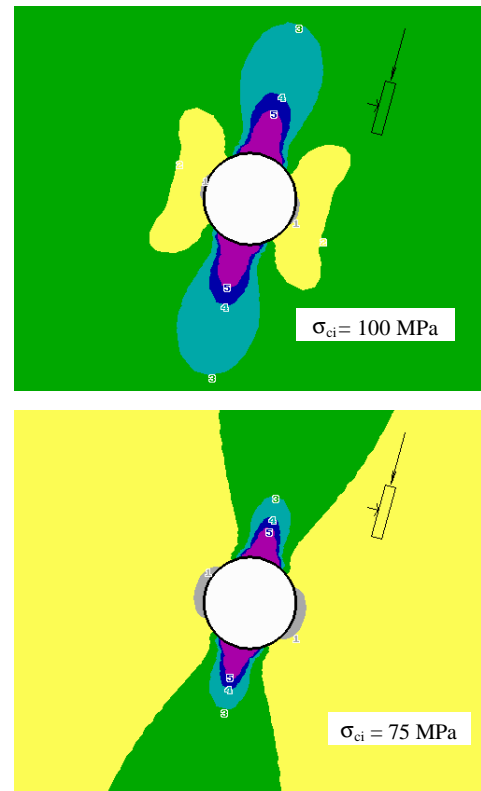


Figure 17. Strength factor contours determined with the  $m = 0$  approach for the tunnel at ch 2360 m ( $s_i = 100, 75$  MPa).

#### 3.5.2. The elastic-brittle-plastic model

The analyses above considered overstressing of the rock mass around the tunnel periphery, without accounting for the presence of discontinuities. Therefore, it was decided to analyse the same instability problem by introducing these features in the numerical model.

As shown in Figure 18, the model comprises two parallel discontinuities near the right sidewall, dipping toward the tunnel. In order to account for the rock mass disturbance due to jointing in the proximity of the discontinuities and the apparently more massive rock on the left sidewall, where relatively little slabbing and overstressing was present, it was decided to introduce three different regions in the model with the following material properties, according to the Hoek-Brown failure criterion:

| Material properties | Region (Figure 18) |       |       |
|---------------------|--------------------|-------|-------|
|                     | 1                  | 2     | 3     |
| $E_m$ [GPa]         | 35                 | 7.5   | 18    |
| $\nu_m$ [-]         | 0.25               | 0.35  | 0.35  |
| $\sigma_{ci}$ [MPa] | 150                | 150   | 150   |
| $m_{tp}$ [-]        | 2.4                | 0.74  | 1.68  |
| $S_b$ [-]           | 0.036              | 0.002 | 0.012 |
| $m_{tr}$ [-]        | 1.2                | 0.74  | 1.00  |
| $S_r$ [-]           | 0.0087             | 0.002 | 0.001 |

for:  $\sigma_{ci}$  = intact rock strength;  $m_{bp}$ ,  $m_{br}$ ,  $s_b$ ,  $s_r$  = Hoek-Brown constants;  $E_m$  = rock mass deformation modulus;  $\nu_m$  = Poisson's ratio.

The rock mass surrounding the tunnel was specified as plastic and the elastic-brittle-plastic option of Phase<sup>2</sup> was activated by specifying the constants for peak strength ( $m_{bp}$ ,  $s_b$ ) different than residual strength ( $m_{br}$ ,  $s_r$ ) only for the more massive rock mass conditions. The values were chosen on the basis of personal judgement with the purpose to account for the better rock mass conditions on the sidewall. The discontinuities were introduced in the model by using the joint option of Phase<sup>2</sup>, with the following joint properties:

| Joint properties | Joint (Figure 19) |      |
|------------------|-------------------|------|
|                  | 1                 | 2    |
| $K_n$ [MPa/m]    | 1250              | 1250 |
| $K_s$ [MPa/m]    | 125               | 125  |
| $h$ [m]          | 0.08              | 0.02 |
| $c$ [MPa]        | 0                 | 0    |
| $\phi$ [°]       | 22                | 22   |

for:  $K_n$ ,  $K_s$  = normal and shear stiffness;  $h$  = joint aperture;  $c$  = joint cohesion;  $\phi$  = joint friction angle.

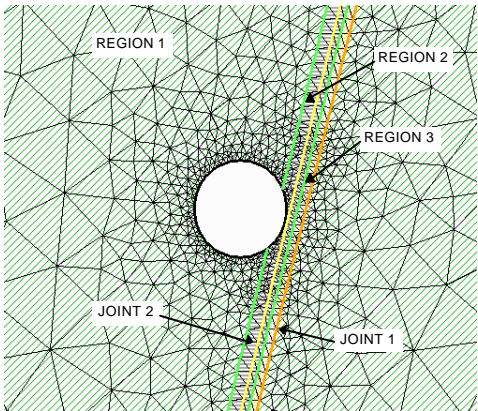


Figure 18. Detail of the FEM model near the tunnel showing regions with different material properties and joints (refer to values in previous tables).

Figure 19 shows the deepening of the failure zones in the right and left walls as predicted by the elastic-brittle-plastic model. The results of such an analysis is the more significant deepening of breakout on the right wall in agreement with observations in the tunnel where stress failure and block movement actually occurred during face advance, resulting in jamming of the TBM.

It is concluded that the structural discontinuities near the tunnel govern to a significant extent the stability conditions. This is a very relevant aspect combined with the high overburden and highly anisotropic stress regime in the present situation, and effect of water, which was not included in the numerical analysis.

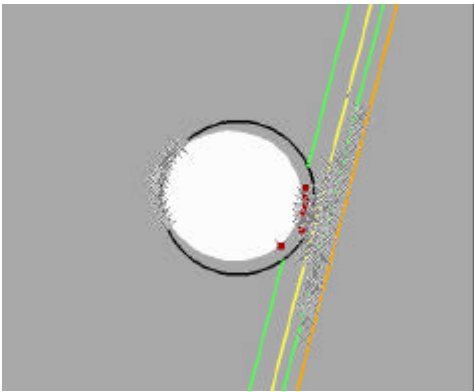


Figure 19. Computed yielded zones around the tunnel and deformed mesh using the elastic-brittle-plastic constitutive model.

### 3.5.3. Lessons learned

The future geological and hydrogeological conditions along the tunnel alignment anticipate the presence of clay filled discontinuities with unfavorable orientation as experienced in the actual situation, with high hydrostatic head.

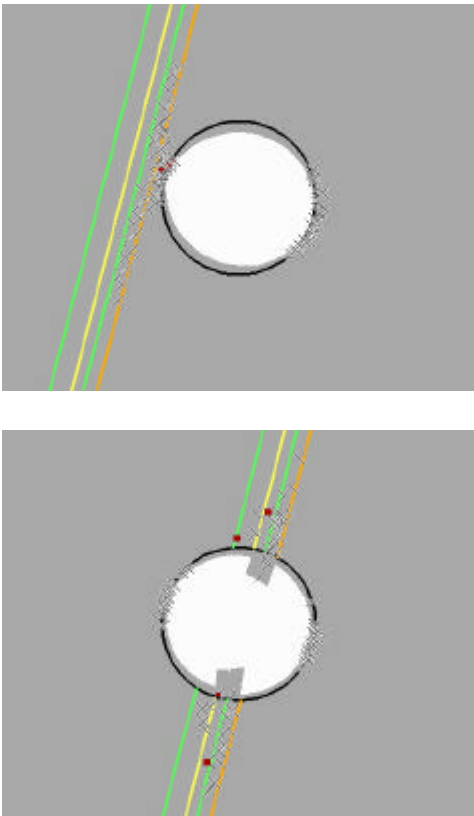


Figure 20. Computed yielded zones around the tunnel and deformed mesh using the elastic-brittle-plastic constitutive model for two possible geological conditions along the tunnel axis.

Then, the lessons learned so far need to be taken into account in order to carefully assess the interactive behaviour between the rock surround and TBM. In fact, the tunnelling conditions could become more problematic, as

they involve already highly stressed rock masses, with the overburden expected to rise up to 800 m maximum.

With this in mind, also considering that the TBM is driven along a curved axis, it is of interest to use the predictive capability of the elastic-brittle-plastic model to analyse two possible scenarios:

- 1) the discontinuities run parallel to the tunnel axis, at the crown;
- 2) the discontinuities are at the left wall.

The analyses were carried out with the same assumptions given above for the material and joint properties and the in situ state of stress. The results obtained are given in Figure 20 by showing the plot of the yielded zones around the tunnel and the deformed mesh.

### 3.6. Discontinuum modelling

With the understanding that discontinuities (major discontinuities and jointing) play a key role in the development of tunnel instability, the problem was also investigated by adopting discontinuous models, with the 2D distinct element code, UDEC (Itasca, 1996). The rock mass surrounding the tunnel was represented by two discontinuous models as follows.

#### 3.6.1. Deterministic model

The rock mass was considered to be intercepted by three sets of joints, and foliation. Different spacing, degree of persistence and shear strength properties were introduced in the model so as to simulate the rock mass conditions away from the fault zone as illustrated in Figure 21. The joints were again assumed to be Mohr-Coulomb joints, i.e. elasto-perfectly plastic joints. The blocks were treated as an elasto-plastic material which follows Mohr-Coulomb criterion. The properties of rock blocks and joints are listed below:

| Material Properties (*) |       | Zone (Figure 8 and 10) |      |      |
|-------------------------|-------|------------------------|------|------|
|                         |       | 1                      | 2    | 3    |
| $E_m$                   | [GPa] | 60                     | 30   | 10   |
| $\nu_m$                 | [-]   | 0.25                   | 0.35 | 0.35 |
| $c$                     | [MPa] | 34                     | 6.0  | 2.8  |
| $\phi$                  | [°]   | 38                     | 36   | 34   |

(\*)  $c$  = cohesion;  $\phi$  = friction angle;  $E_m$  = rock mass deformation modulus;  $\nu_m$  = Poisson's ratio.

| Joint Properties (*) |         | Zone (Figure 8 and 10) |                    |                     | Joint (Figure 8 and 10) |  |
|----------------------|---------|------------------------|--------------------|---------------------|-------------------------|--|
|                      |         | 1                      | 2                  | 3                   | 1 - 2                   |  |
| $K_n$                | [GPa/m] | 40                     | $5 \times 10^{-3}$ | $10 \times 10^{-3}$ | $1.25 \times 10^{-3}$   |  |
| $K_s$                | [GPa/m] | 4                      | $5 \times 10^{-4}$ | $10 \times 10^{-4}$ | $1.25 \times 10^{-4}$   |  |
| $c$                  | [MPa]   | 0.1                    | 0                  | 0                   | 0                       |  |
| $\phi$               | [°]     | 33                     | 22                 | 22                  | 22                      |  |

(\*)  $K_n$ ,  $K_s$  = normal and shear stiffness;  $c$  = joint cohesion;  $\phi$  = joint friction angle.

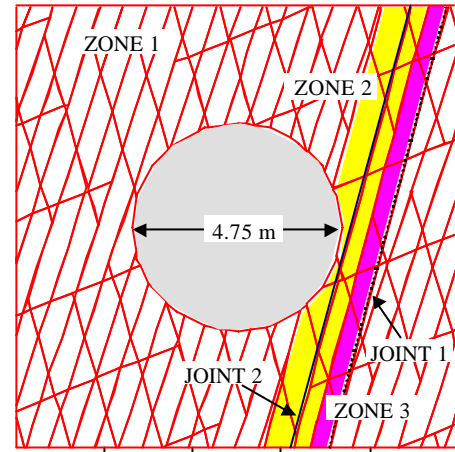


Figure 21. Detail of UDEC deterministic model showing regions with different material and joint properties.

#### 3.6.2. Discrete Feature Network (DFN) model

A Discrete Feature Network model was also created by using the procedures implemented in the FracMan code (Dershowitz et al., 1995). The results of geologic mapping on the right wall of the tunnel formed the basis for defining the input data in terms of orientation, size and degree of fracturing for the joint sets J1, J2 and J3 a, b. These were superimposed with foliation and discrete features represented by the two sub-parallel discontinuities described above. The 3D volume realized in this way is shown in Figure 22, where also shown is the plot of the joint sets given with the FracMan code.

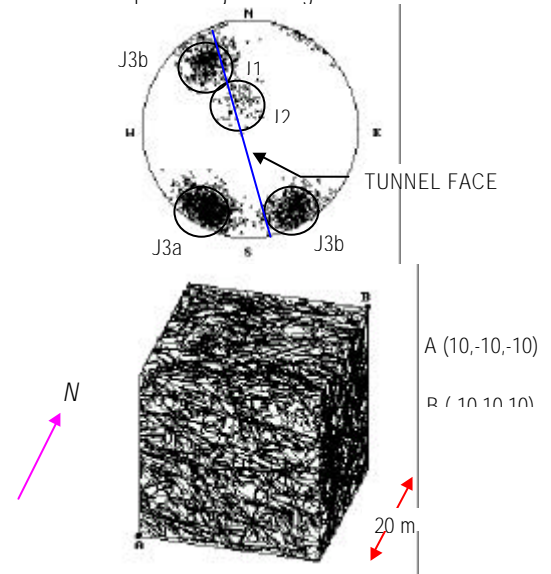


Figure 22. 3D Discrete Feature Network model created by the FracMan code with plot of joint sets. This is typical for rock conditions on the right wall.

The UDEC model was obtained by taking a cross section orthogonal to the tunnel axis through the 3D DFN volume of Figure 22. This network of 2D fractures is not directly amenable to UDEC analysis as the fractures need to be well connected and no isolated fractures can be handled by the code. At the same time, it was necessary to cross-validate the model against the rock mass conditions around the tunnel. This was carried out by

increasing the block size in the original 2D network model both at the crown and on the left wall, to account for the generally better rock mass conditions in these zones.

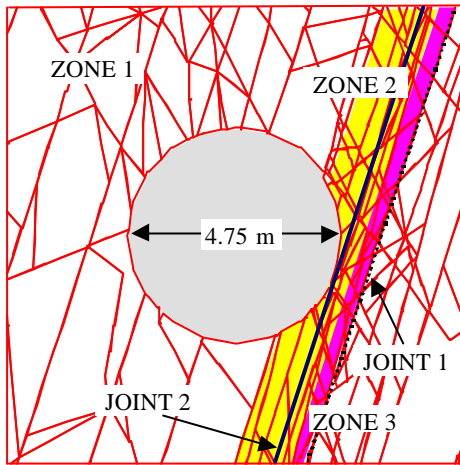


Figure 23. Detail of UDEC-DFN model showing regions with different material properties and joints.

A random process which cancels the fracture traces exceeding a given limit-length fixed was used in conjunction with the *Set edge* command which is available with the UDEC code. A typical model finally developed is shown in Figure 23. As for the deterministic model described above, the joints were assumed to behave as Mohr-Coulomb joints and the blocks were treated as an elasto-plastic material. The input data are the same as listed above and shown in Figure 21.

### 3.6.3. Results

For both the deterministic and DFN models the same stress conditions as assumed for the continuum models were applied.

In order to investigate whether the continuum approach can yield similar results to the discontinuum approach, the calculations were carried to simulate tunnel excavation as for the finite element models by using stress boundary conditions. Also, no account was taken for the water pressure distributed around the tunnel. The main interest was posed on the yield zones, as shown by blocks which are failing, and on shear displacements induced along joints (Figure 24). Attention was also paid to the pattern of block movements at the right wall (Figure 25).

The results obtained show that both the deterministic and DFN models capture well the overstressing conditions and block movements of right wall. As for the elastic-brittle-plastic model which accounts for the presence of the two sub-parallel discontinuities, the deepening of breakout on the right wall is well reproduced with the discontinuum approach (compare Figure 19 with Figure 24). However, in the latter case (Figure 24) no significant instability is seen to develop at the left wall, unlike the continuum approach (Figure 19). The similarity is evident with the actual conditions in the tunnel, where the TBM jammed because of instability and block movement at the right wall (Figures 14 and 15).

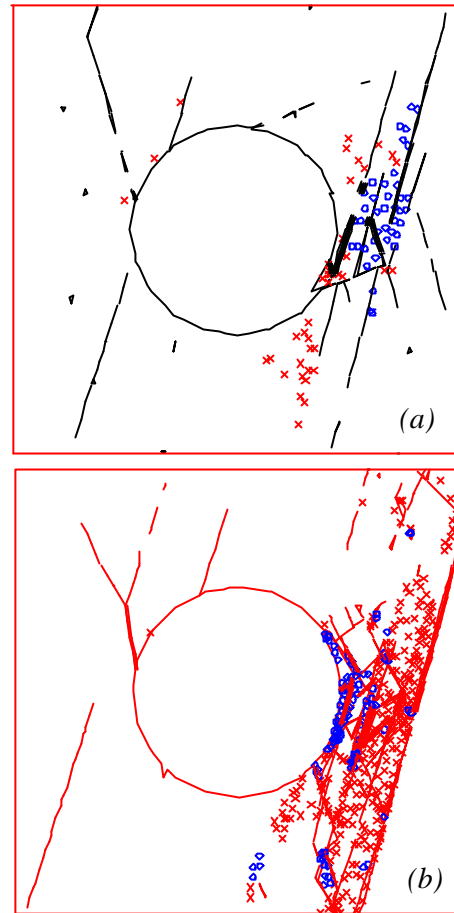


Figure 24. Yielded blocks and shear displacements along the joints around the tunnel; (a) deterministic model, (b) DFN model.

The continuum approach appears to capture some of the adverse factors which were significant in the instability conditions that developed during TBM excavation:

- the elastic-plastic-brittle behaviour of rock material,
- the highly anisotropic stress regime with a very low stress ratio,
- the presence of unfavourable dominant discontinuities at the right wall.

In comparison, the discontinuum approach shows in a remarkable manner the block movement developing on the right wall, whereas the tunnel remains stable along the periphery away from the fault zone at the crown and right wall.

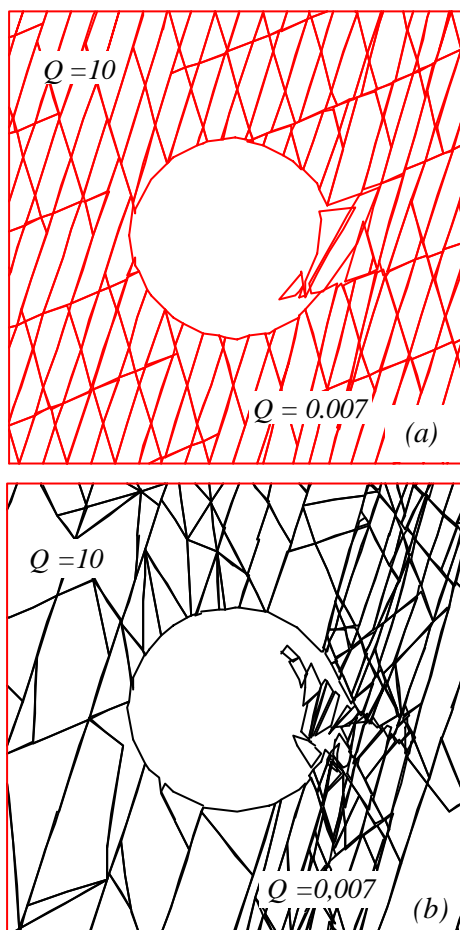


Figure 25. Block movements around the tunnel; (a) deterministic model, (b) DFN model.

## 4. CONCLUSIONS

Modern numerical modelling methods by the use of either the equivalent continuum or discontinuum approach have been discussed by underlying some of the fundamental concepts and guidelines, when investigating tunnel problems at the design analysis stage. With reference to modelling in engineering practice, the interest has been placed on the adoption of discontinuum models which give a far more realistic and representative picture of rock mass behaviour than equivalent continuum models.

Modelling of rock mass around a 4.75 m diameter tunnel excavated by an open TBM configuration through quartzitic micaschists has been described, with attention paid to the instability conditions that developed when crossing through a fault zone. The calculations were performed by using the finite element method and the distinct element method, according to a two dimensional modelling format, three-dimensional representation being too limited and not justifiable in respect of the uncertainties of the input data.

With the finite element method an equivalent continuum approach was applied, including the influence of two major discontinuities on the right wall. With the distinct element method a fully discontinuum approach was used by either a deterministic or discrete feature network model. The discontinuum representation of the rock mass captures in a remarkable manner the instability conditions that developed at the TBM head during excavation. In

comparison, the continuum representation gives a more idealised illustration of the instability. It is concluded that for stability analysis peculiar geologic conditions such as fault zones around the tunnel require specific models, which reflect the given conditions in the most realistic way possible.

## 5. REFERENCES

- Barla G., M. Barla, L. Repetto 1999. *Continuum and discontinuum modelling for design analysis of tunnels*. 9<sup>th</sup> Int. Congr. on Rock Mech. Paris, France.
- Bandis S. 1993. *Engineering properties and characterization of rock discontinuities*. Comprehensive Rock Engineering. Volume 1. Fundamentals (Hudson J.A., editor). pp. 155-183. Pergamon Press, Oxford (UK).
- Barton N., R. Lien, J. Lunde 1974. *Engineering classification of jointed rock masses for the design of tunnel support*. Rock Mechanics. Vol. 6, pp. 189-236.
- Barton N. 1997. Pont Ventoux Hydropower Project. Tunnel F2 - Pont Ventoux. *Assessment of geological conditions and required support for ch 2350-4000*. Report to Nocon. 25 October 1997.
- Barton N. 1998. *Quantitative description of rock masses for the design of NMT reinforcement (Special Lecture 1)*. Int. Conf. on Hydro Power Development In Himalayas. Shimla, India.
- Barton N. 1999. *General report concerning some 20<sup>th</sup> century lessons and 21<sup>st</sup> century challenges in applied rock mechanics*. 9<sup>th</sup> International Congress on Rock Mechanics. August 25 – 28, 1999, Paris.
- Brown E.T., J.W. Bray, B. Ladanyi, E. Hoek 1983. *Characteristic line calculations for rock tunnels*. J. Geotech. Eng. Div. Am. Soc. Civ. Engrs. 109. pp. 15-39.
- Cundall P.A., R.D. Hart 1993. *Numerical modelling of discontinua*. Comprehensive Rock Engineering. Volume 2. Analysis and Design Methods (Hudson J.A., editor). pp. 231-261. Pergamon Press, Oxford (UK).
- Curran J. H. and Corkun B. T. 1997. Phase<sup>2</sup>. 2D finite element program for calculating stresses and estimating support around underground excavations. *Reference Manual and Tutorial Manual*. Rock Engineering Group. University of Toronto.
- Dershowitz, W., G. Lee, J. Geier, P. La Pointe 1995. *FracMan Interactive Discrete Feature Data Analysis, Geometric Modelling and Exploration Simulation*. User documentation. Version 2.50. Seattle. Golder Associates Inc.
- Grimstad E., N. Barton 1993. *Updating the Q-system for NMT*. Proc. of Int. Symp. on Sprayed Concrete. Modern use of wet mix sprayed concrete for underground support. Fagernes (Kompan, Opsahl and Berg, editors). Norwegian Concrete Association. Oslo.
- Hart R.D. 1993. *An introduction to distinct element modelling for rock engineering*. Comprehensive Rock Engineering. Volume 2. Analysis and Design Methods (Hudson J.A., editor). pp. 245-263. Pergamon Press, Oxford (UK).
- Hoek E., M.W. Grubinsky, M.S. Diederichs 1991. *Numerical modelling for underground excavation design*. Trans. Inst. Min. Metal. Vol. 100. January-April 1991, pp. A22-A30.
- Hoek E., E.T. Brown 1997. *Practical estimates of rock mass strength*. Int. J. Rock Mech. Min. Sci. Vol. 34, pp. 1156-1186.



- Itasca Consulting Group 1996. *UDEC (Universal Distinct Element Code), version 3.0. Volume I: User's manual. Volume II: Verification problems and example applications.* Minneapolis, Minnesota, USA.
- Martin C. D., D.R. Mc Creath, M. Stochmal 1997. *Estimating support demand-load caused by stress-induced failure around tunnels.* Int. Symp. on Rock Support, Lillehammer, June 1997.
- Panet M. 1995. *Le calcul des tunnels par la méthode convergence-confinement.* Presses de l'Ecole Nationale des Ponts et Chaussées.
- Pont Ventoux 1997. *Nota relativa al sopralluogo effettuato in data 8/10/1997 in corrispondenza del fronte di scavo della galleria di derivazione nel tratto Pont Ventoux - F2 (Dott. Geol. G. Venturini).*
- Shen B., N. Barton 1997. *The disturbed zone around tunnels in jointed rock masses.* Int. J. Rock Mech. Min. Sci. Vol. 34, pp. 117-125.
- Startfield A.M., Cundall P.A. 1988. *Towards a methodology for rock mechanics modelling.* Int. J. Rock Mech. Min. Sci. Vol. 25, pp. 99-106.

## 6. ACKNOWLEDGEMENTS

The work described in this paper was carried out with the financial support of the Italian Ministry for University and Technological Research (M.U.R.S.T.) as part of the Research Programme "Tunnelling in difficult conditions" (40%). The authors would like to acknowledge the help of G. Giampieri and L. Repetto, former students at the Politecnico di Torino.

The permission of AEM (Azienda Energetica Metropolitana) Torino, owner of the Pont Ventoux-Susa Hydropower Project, to publish this paper on the F2 tunnel is gratefully acknowledged. The authors would also like to thank the following companies involved in the project described in the paper: Astaldi S.p.A., Italy and Nocon, Norway.